

Deuteron electromagnetic form factors in transverse plane with a phenomenological Lagrangian approach

Cuiying Liang^{1,2,3}, Yubing Dong^{1,2}, and Weihong Liang³

¹ *Institute of High Energy Physics,
Chinese Academy of Sciences,
Beijing 100049, P. R. China*

² *Theoretical Physics Center for Science Facilities (TPCSF), CAS, P. R. China
and*

³ *College of Physical Science and Technology,
Guangxi Normal University,
Guilin 541004, P. R. China*

(Dated: February 19, 2018)

A phenomenological Lagrangian approach is employed to study the electromagnetic properties of deuteron. The deuteron is regarded as a loosely bound state of a proton and a neutron. The deuteron electromagnetic form factors are expressed in light-front representation in the transverse plane. The transverse charge density of the deuteron is discussed.

PACS numbers: 13.40.Gp, 14.20.Dh, 36.10.Gv

Keywords: deuteron, nucleon, electromagnetic form factors, transverse plane, impact parameter space

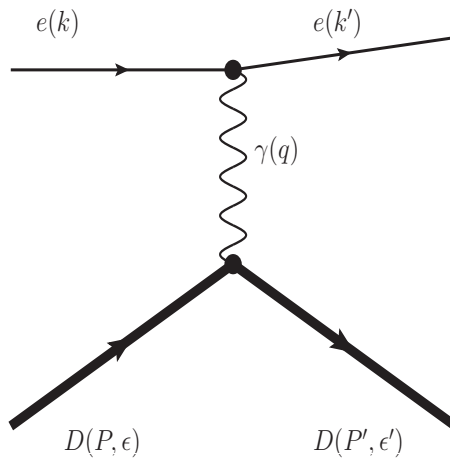


FIG. 1. Feynman diagram for electron-deuteron elastic scattering in the one-photon approximation.

I. INTRODUCTION

It is known that the study of electromagnetic(EM) form factors of proton, neutron and light nuclei, like deuteron and He-3, is crucial for the understanding of nucleon structures. It tells the distributions of the charge and magnetization inside systems. The EM form factors of the deuteron have been explicitly discussed (for some recent reviews, see, e.g. [1]-[4]) for several decades. A deuteron, as a spin-1 particle, has three form factors of charge G_C , magnetic G_M , and quadrupole G_Q . It is often regarded as a loosely bound state of the proton and neutron (with binding energy $\epsilon_D \sim 2.22$ MeV), and consequently the study of the deuteron properties can shed light on the structure of the nucleon as well as nuclear effects. Moreover, it is found that the two constituents – proton and neutron inside the deuteron are dominated by the relative S -wave, and the D -wave is only about 5%. The understanding of the deuteron structures, like its EM form factors and its binding energy, is usually based on potential models, on phenomenological models with quark, meson, and nucleon degrees of freedom, and on some effective field theories etc. [1–12]. The realistic deuteron wave function has already been explicitly given by Ref. [13], particularly, the relativistic deuteron wave function was discussed and obtained in Refs. [14–16].

Recently, the pion transverse charge density $\rho_C(b)$ is of great interests. It stands for the two-dimensional Fourier transform of the EM form factor and for the density (in the infinite momentum frame) located at a transverse separation b (impact parameter) from the center of transverse momentum [17–21]. It is pointed out that this two-dimensional density can directly relate to the matrix element of a density operator. However, the usual three-dimensional Fourier transforms of the form factors cannot, since the initial and final momentums are different and one cannot boost the initial and final states to the rest frame simultaneously. There are also many discussions on the proton EM form factors in the transverse plane.

Analogous to pion, in this paper, we will study the EM form factors of the deuteron in the transverse plane. A phenomenological approach will be employed for the deuteron, where it is regarded as a loosely bound state of a proton and a neutron and the two constituents are in relative S -wave. The coupling of the deuteron to its two composite particles is determined by the known compositeness condition from Weinberg [22], Salam [23] and others [24, 25]. Our approach has been successfully applied to study the properties of weakly bound state problems, like the new resonances of $X(3872)$, $\Lambda_c(2940)$, and the EM form factors of pion as well as some other observables [26, 27].

This paper is organized as follows. In section II, the general properties of the deuteron (spin-1 particle) is briefly reviewed, and moreover, our phenomenological approach is briefly explained. In section III, the EM form factors of the deuteron in the light-front representation are given. Our numerical results for the EM form factors in the transverse plane are shown in section IV. Finally, section V is devoted for a short summary.

II. OUR FRAMEWORK

A. Deuteron electromagnetic form factors

A deuteron is a spin-1 particle, and its EM properties can be explored by a lepton-deuteron elastic scattering. The matrix element for electron-deuteron (eD) elastic scattering in the one-photon approximation, as shown in Fig. 1, can be written as

$$\mathcal{M} = \frac{e^2}{Q^2} \bar{u}_e(k') \gamma_\mu u_e(k) \mathcal{J}_\mu^D(P, P'), \quad (1)$$

where k and k' are the four-momenta of initial and final electrons. $\mathcal{J}_\mu^D(P, P')$ is the deuteron EM current, and its general form is

$$\mathcal{J}_\mu^D(P, P') = - \left(G_1(Q^2) \epsilon'^* \cdot \epsilon - \frac{G_3(Q^2)}{2M_D^2} \epsilon \cdot q \epsilon'^* \cdot q \right) (P + P')_\mu - G_2(Q^2) \left(\epsilon_\mu \epsilon'^* \cdot q - \epsilon'_\mu \epsilon \cdot q \right), \quad (2)$$

where M_D is the deuteron mass, $\epsilon(\epsilon')$ and $P(P')$ are polarization and four-momentum of the initial (final) deuteron, and $Q^2 = -q^2$ is momentum transfer square with $q = P' - P$. The three EM form factors $G_{1,2,3}$ of the deuteron are related to the charge G_C , magnetic G_M , and quadrupole G_Q form factors by

$$G_C = G_1 + \frac{2}{3}\tau G_Q, \quad G_M = G_2, \quad G_Q = G_1 - G_2 + (1 + \tau)G_3, \quad (3)$$

with $\tau = \frac{Q^2}{4M_D^2}$. The three form factors are normalized at zero recoil as

$$G_C(0) = 1, \quad G_Q(0) = M_D^2 \mathcal{Q}_D = 25.83, \quad G_M(0) = \frac{M_D}{M_N} \mu_D = 1.714, \quad (4)$$

where M_N is the nucleon mass, \mathcal{Q}_D and μ_D are the quadrupole and magnetic moments of the deuteron.

The unpolarized differential cross section for the eD elastic scattering can be expressed by the two structure functions, $A(Q^2)$ and $B(Q^2)$, as

$$\frac{d\sigma}{d\Omega} = \sigma_M \left[A(Q^2) + B(Q^2) \tan^2 \left(\frac{\theta}{2} \right) \right], \quad (5)$$

where $\sigma_M = \alpha^2 E' \cos^2(\theta/2) / [4E^3 \sin^4(\theta/2)]$ is the Mott cross section for point-like particle, E and E' are the incident and final electron energies, θ is the electron scattering angle, $Q^2 = -q^2 = 4EE' \sin^2(\theta/2)$, and $\alpha = e^2/4\pi = 1/137$ is the fine-structure constant. The two form factors $A(Q^2)$ and $B(Q^2)$ are related to the three EM form factors of the deuteron as

$$A(Q^2) = G_C^2(Q^2) + \frac{8}{9}\tau^2 G_Q^2(Q^2) + \frac{2}{3}\tau G_M^2(Q^2), \quad B(Q^2) = \frac{4}{3}\tau(1 + \tau)G_M^2(Q^2). \quad (6)$$

Clearly, the three form factors $G_{C,M,Q}$ cannot be simply determined by measuring the unpolarized elastic eD differential cross section. To uniquely determine the three form factors of the deuteron one additional polarization variable is necessary. For example, one may take the polarization of T_{20} [4]

$$T_{20} = -\frac{1}{\sqrt{2}\mathcal{S}} \left\{ \frac{8}{3}\tau G_C G_Q + \frac{8}{9}\tau^2 G_Q^2 + \frac{1}{3}\tau [1 + 2(1 + \tau) \tan^2(\theta/2)] G_M^2 \right\}, \quad (7)$$

into account, where $\mathcal{S} = A + B \tan^2(\theta/2)$.

B. The phenomenological approach

Here we will briefly show the formalisms of the phenomenological approach. Take an assumption that the deuteron is interpreted as a hadronic molecule – a weakly bound state of the proton and neutron: $|D\rangle = |pn\rangle$ (see Fig. 2), then

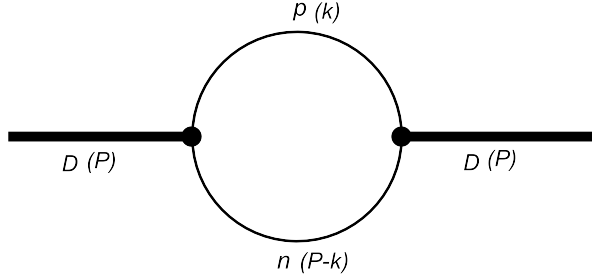


FIG. 2. Deuteron mass operator

one may simply write a phenomenological effective Lagrangian of the deuteron and its two constituents – proton and neutron, as

$$\mathcal{L}_D(x) = g_D D_\mu^\dagger(x) \int dy \bar{p}^c(x + y/2) \tilde{\Phi}_D(y^2) \Gamma^\mu n(x - y/2) + H.c., \quad (8)$$

where D_μ is the deuteron field, $\bar{p}^c(x) = p^T(x)C$, C denotes the matrix of charge conjugation, and x is the centre-of-mass (C. M.) coordinate. In Eq. (8), $\tilde{\Phi}_D(y^2)\Gamma^\mu$ is the vertex where the correlation function $\tilde{\Phi}_D(y^2)$ characterizes the finite size of the deuteron as a pn bound state and depends on the relative Jacobi coordinate y .

A basic requirement for the choice of an explicit form of this correlation function is that its Fourier transform vanishes sufficiently fast in the ultraviolet region of Euclidean space to render the Feynman diagrams ultraviolet finite. Usually a Gaussian-type function is selected as the correlation for simplicity. One chooses

$$\tilde{\Phi}_D(k^2)\Gamma^\mu = \exp(-k_E^2/\Lambda_D^2)\gamma^\mu, \quad (9)$$

for the Fourier transform of the correlation function, where $\Gamma^\mu = \gamma^\mu$, k_E is the Euclidean Jacobi momentum and Λ_D is a free size parameter which represents the distribution of the two constituents in the deuteron.

The coupling of g_D in Eq. (8) can be determined by the known compositeness condition, which implies the renormalization constant of the hadron wave function is set equal to zero as $Z_D = 1 - \Sigma'_D(M_D^2) = 0$, with $\Sigma'_D(M_D^2) = g_D^2 \Sigma'_{D\perp}(M_D^2)$ being the derivative of the transverse part of the mass operator (see Fig. 2). Usually, the mass operator splits into the transverse part $\Sigma_{D\perp}(k^2)$ and longitudinal one $\Sigma_{D\parallel}(k^2)$ as

$$\Sigma_D^{\alpha\beta}(k) = g_\perp^{\alpha\beta} \Sigma_{D\perp}(k^2) + \frac{k^\alpha k^\beta}{k^2} \Sigma_{D\parallel}(k^2), \quad (10)$$

where $g_\perp^{\alpha\beta} = g^{\alpha\beta} - k^\alpha k^\beta / k^2$ and $g_\perp^{\alpha\beta} k_\alpha = 0$. From Eqs. (9-10) we see that for a fixed parameter Λ_D , the coupling of the deuteron to its constituents – proton and neutron, g_D , is well determined by the compositeness condition. The explicit expression of g_D (in the simplest case of Eq. (8)), in terms of the loop integral shown in Fig. 2, has been given in Refs. [27, 28]. The correlation function of Eq. (9) simulates only the S -wave in the deuteron. It is commonly believed that the relative S -wave is dominant in the deuteron.

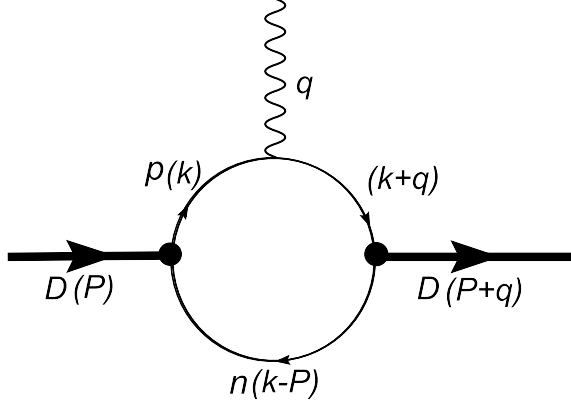


FIG. 3. Electron-deuteron scattering diagram contributing to the EM form factors.

III. THE LIGHT-FRONT REPRESENTATION

A. EM form factors in the light-front representation

To study the EM properties of the deuteron, we assume the deuteron as a bound state of the proton and neutron. Therefore, the eD scattering can be interpreted as the photon coupling respectively to the proton and neutron, as shown in Fig. 3. The general expression of the loop integral of Fig. 3 is

$$i\mathcal{M}^\alpha = i\epsilon_\mu^* \mathcal{M}^{\alpha\mu\nu} \epsilon_\nu \quad (11)$$

where

$$\begin{aligned} \mathcal{M}^{\alpha\mu\nu} = & -ig_D^2 \int \frac{d^4k}{(2\pi)^4} \frac{\text{Tr}[\gamma^\mu(\not{k} + \not{q} + M_N)\Gamma^\alpha(\not{k} + M_N)\gamma^\nu(\not{k} - \not{P} + M_N)]}{(k^2 - M_N^2)[(k+q)^2 - M_N^2][(k-P)^2 - M_N^2]} \\ & \times \tilde{\Phi}_D((k-P/2)_E^2) \tilde{\Phi}_D((k-P/2+q/2)_E^2), \end{aligned} \quad (12)$$

and

$$\Gamma^\alpha = \gamma^\alpha [F_1^p(Q^2) + F_1^n(Q^2)] + i \frac{\sigma^{\alpha\beta} q_\beta}{2M_N} [F_2^p(Q^2) + F_2^n(Q^2)], \quad (13)$$

where $F_{1,2}^{p,n}$ are the Dirac and Pauli form factors of the proton and neutron, respectively. In Eq. (12), $\tilde{\Phi}_D$ stands for the correlation function.

With the help of the calculation of the scalar loop integral of $I(P^2, q^2, P \cdot q)$ shown in appendix, one may easily compute the matrix element $\mathcal{M}^{\alpha\mu\nu}$ in Eq. (12) in the light-front representation. Furthermore, one may obtain the model-dependent deuteron form factors according to the general Lorentz structure given by Eq. (2). Taking the

charge form factor of the deuteron for example, the obtained form factor is

$$\begin{aligned}
G_C(Q^2) = g_D^2 \sum_{N=p,n} \int \frac{dx d^2 \vec{k}}{(2\pi)^3} \frac{2[M_D^2(1+x) + xQ^2 + \vec{k} \cdot \vec{q}] F_1^N(Q^2) - Q^2 F_2^N(Q^2)}{x^2(1-x) \left[P^+ P^- - \frac{\vec{k}^2 + M_N^2}{x} - \frac{(\vec{k} - \vec{P})^2 + M_N^2}{1-x} \right] \left[P^+ P^- - \frac{(\vec{k} + \vec{q})^2 + M_N^2}{x} - \frac{(\vec{k} - \vec{P})^2 + M_N^2}{1-x} \right]} \quad (14) \\
\times \exp \left[-\frac{1}{\Lambda_D^2} \left(x - \frac{1}{2} \right) \left[\frac{P^+ P^-}{2} - \frac{(\vec{k} - \frac{\vec{P}}{2})^2}{x - \frac{1}{2}} - \frac{(\vec{k} - \vec{P})^2 + M_N^2}{1-x} \right] \right] \\
\times \exp \left[-\frac{1}{\Lambda_D^2} \left(x - \frac{1}{2} \right) \left[\frac{P^+ P^-}{2} - \frac{(\vec{k} - \frac{\vec{P}}{2} + \frac{\vec{q}}{2})^2}{x - \frac{1}{2}} - \frac{(\vec{k} - \vec{P})^2 + M_N^2}{1-x} \right] \right],
\end{aligned}$$

where $P^\pm = P^0 \pm P^3$, and $x = k^+ / P^+$. In addition, we define the transverse momentum

$$\vec{\kappa} = (1-x)\vec{k} - x(\vec{P} - \vec{k}) = \vec{k} - x\vec{P}, \quad (15)$$

then the charge form factor can be re-written as

$$\begin{aligned}
G_C(Q^2) = g_D^2 \sum_{N=p,n} \int \frac{dx d^2 \vec{\kappa}}{(2\pi)^3} \frac{[2M_D^2(1+x) + \vec{\kappa} \cdot \vec{q}] F_1^N(Q^2) - Q^2 F_2^N(Q^2)}{x^2(1-x) \left[M_D^2 - \frac{\vec{\kappa}^2 + M_N^2}{(1-x)x} \right] \left[M_D^2 - \frac{[\vec{\kappa} + (1-x)\vec{q}]^2 + M_N^2}{(1-x)x} \right]} \quad (16) \\
\times \exp \left[\frac{1}{\Lambda_D^2} \left(x - \frac{1}{2} \right) \left(\frac{M_D^2}{2} - \frac{M_N^2}{1-x} - \frac{\vec{\kappa}^2}{2(x - \frac{1}{2})(1-x)} \right) \right] \\
\times \exp \left[\frac{1}{\Lambda_D^2} \left(x - \frac{1}{2} \right) \left(\frac{M_D^2}{2} - \frac{M_N^2}{1-x} - \frac{[\vec{\kappa} + (1-x)\vec{q}]^2}{2(x - \frac{1}{2})(1-x)} \right) \right].
\end{aligned}$$

Let us define a wave function ψ as

$$\psi(x, \vec{\kappa}) = \frac{1}{M_D^2 - \frac{\vec{\kappa}^2 + M_N^2}{(1-x)x}} \exp \left[\frac{1}{\Lambda_D^2} \left(x - \frac{1}{2} \right) \left(\frac{M_D^2}{2} - \frac{M_N^2}{1-x} - \frac{\vec{\kappa}^2}{2(x - \frac{1}{2})(1-x)} \right) \right], \quad (17)$$

and finally the charge form factor is

$$\begin{aligned}
G_C(Q^2) = g_D^2 \sum_{N=p,n} \int \frac{dx d^2 \vec{\kappa}}{(2\pi)^3 x^2 (1-x)} \left\{ [2M_D^2(1+x) + \vec{\kappa} \cdot \vec{q}] F_1^N(Q^2) - Q^2 F_2^N(Q^2) \right\} \psi(x, \vec{\kappa}) \quad (18) \\
\times \psi^*(x, \vec{\kappa} + (1-x)\vec{q}).
\end{aligned}$$

In the same way, the magnetic form factor is

$$\begin{aligned}
G_M(Q^2) = g_D^2 \sum_{N=p,n} \int \frac{dx d^2 \vec{\kappa}}{(2\pi)^3 x^2 (1-x)} \left\{ [2M_D^2(1+3x) - 6\frac{\vec{\kappa}^2 + M_N^2}{1-x} + 8M_N^2] F_1^N(Q^2) \quad (19) \right. \\
\left. - [2M_D^2(1+2x) - 4\frac{\vec{\kappa}^2 + M_N^2}{1-x} + 4M_N^2] F_2^N(Q^2) \right\} \psi(x, \vec{\kappa}) \psi^*(x, \vec{\kappa} + (1-x)\vec{q}).
\end{aligned}$$

B. Electromagnetic form factors and transverse densities

So far the form factor $G_C(Q^2)$ is expressed by a three-dimensional integration that involves wave functions in momentum-space (see Eqs. (17-19)). The two-dimensional Fourier transform of the wave function of Eq. (17) can be expressed as

$$\begin{aligned}
\psi(x, \mathbf{B}) = \frac{1}{\sqrt{(1-x)x^2}} \int \frac{d^2 \vec{\kappa}}{(2\pi)^2} \psi(x, \vec{\kappa}) e^{i\vec{\kappa} \cdot \mathbf{B}} \quad (20) \\
= \frac{\sqrt{1-x}}{2\pi} \int_0^\infty dt \frac{\cos |B|t}{\sqrt{t^2 + c^2}} \left(1 - \Phi \left[\sqrt{\frac{t^2 + c^2}{2\Lambda_D^2(1-x)}} \right] \right) \exp \left[\frac{1}{\Lambda_D^2} \left(M_N^2 - \frac{M_D^2}{4} \right) \right],
\end{aligned}$$

where $\Phi(x)$ is error function and $c^2 = M_N^2 - M_D^2(1-x)x$. Thus, the charge form factor of Eq. (18) is expressed as

$$G_C(Q^2) = g_D^2 \sum_{N=p,n} \int_0^1 dx \int \frac{d^2\mathbf{B}}{(2\pi)^3} \left\{ 2[M_D^2(1+x) - (1-x)Q^2] F_1^N(Q^2) - Q^2 F_2^N(Q^2) \right\} |\psi(x, B)|^2 e^{-i\vec{q}\cdot(1-x)\mathbf{B}}. \quad (21)$$

In order to further simplify the expression of $G_C(Q^2)$, the relative transverse position variable \mathbf{B} is expressed by the value of $\mathbf{b}_1 = \mathbf{b}$, which is the transverse position variable of the charged parton of the deuteron. We have

$$\mathbf{B} = \mathbf{b}_1 - \mathbf{b}_2 = \frac{\mathbf{b}}{1-x}, \quad \mathbf{b}_1(x) + \mathbf{b}_2(1-x) = 0. \quad (22)$$

With the help of Eqs. (21-22), we find

$$G_C(Q^2) = \int_0^1 \frac{g_D^2 dx}{1-x} \int \frac{d^2\mathbf{b}}{(2\pi)^3} \sum_{N=p,n} \left\{ 2[M_D^2(1+x) - (1-x)Q^2] F_1^N(Q^2) - Q^2 F_2^N(Q^2) \right\} \left| \psi\left(x, \frac{b}{1-x}\right) \right|^2 e^{-i\vec{q}\cdot\mathbf{b}} \quad (23)$$

The Fourier transform of the charge form factor is

$$G_C(Q^2) = \frac{1}{(2\pi)^2} \int d^2\mathbf{b} \rho_C(b) e^{-i\vec{q}\cdot\mathbf{b}}, \quad (24)$$

where the quantity $\rho_C(b)$ stands for the transverse charge density of the deuteron and b is the impact parameter in the transverse plane. Similarly, one may also determine the transverse magnetic density in the transverse plane as

$$G_M(Q^2) = \frac{1}{(2\pi)^2} \int d^2\mathbf{b} \rho_M(b) e^{-i\vec{q}\cdot\mathbf{b}}, \quad (25)$$

where quantity $\rho_M(b)$ is expressed in terms of the impact parameter b .

IV. NUMERICAL RESULTS

After integrating over x and \mathbf{b} , we may estimate the obtained $G_C(Q^2)$ and $G_M(Q^2)$. In our numerical calculations, the only one model-dependent parameter is Λ_D and we select $\Lambda_D \sim 0.23 \text{ GeV}$ [34]. In Figs. 4 and 5 our numerical results for the charge and magnetic form factors of the deuteron are shown. In order to compare our results with the experimental measurement, the phenomenological parameterizations [29] of the measured two form factors are shown by solid lines in the two figures.

Figs. 4 and 5 show that the present approach could, at least qualitatively, reproduce the EM form factors of the deuteron in the low Q^2 region, although there are discrepancies between our results and the parameterized form factors. The discrepancies become larger when the Q^2 increases. This phenomenon is not surprising. This is due to the fact that our present approach is rather simple and we have only one parameter Λ_D . Moreover, we have employed the Gauss-like correlation function of Eq. (9) to simplify the deuteron wave function for the calculation. However the Gauss-like wave function usually drops faster than the realistic case [29]. It should be mentioned that in order to get the best fits for the deuteron EM form factors, 4 free parameters are employed for each of the three form factors in the parameterization scheme of Ref. [29], just as it claimed that the dipole electric and magnetic form factors of the proton and neutron as well as the meson cloud effect (of ρ and ω mesons) are considered simultaneously in [29]. There are several sets of the parameterization in Ref. [29]. They can reproduce the data in the low Q^2 region quite well.

The important quantities of the present calculation are the transverse charge and magnetic densities $\rho_{C,M}(b)$ of the deuteron. They are written in terms of the impact parameter b in the transverse plane and they stand for the charge and magnetic densities of the deuteron in the transverse plane. In Figs. 6 and 7, we plot the estimated $\rho_{C,M}(b)$ comparing to the results from the parameterized form factors, where the red solid curves and the black dashed curves are obtained from the two-dimensional Fourier transform of the parameterized charge and magnetic form factors [29] as

$$\begin{aligned} \rho_{C,M}(b) &= \int \frac{d^2q}{(2\pi)^2} G_{C,M}(\vec{q}^2) e^{i\vec{q}\cdot\vec{b}} \\ &= \int_0^\infty \frac{qdq}{2\pi} G_{C,M}(\vec{q}^2) J_0(qb), \end{aligned} \quad (26)$$

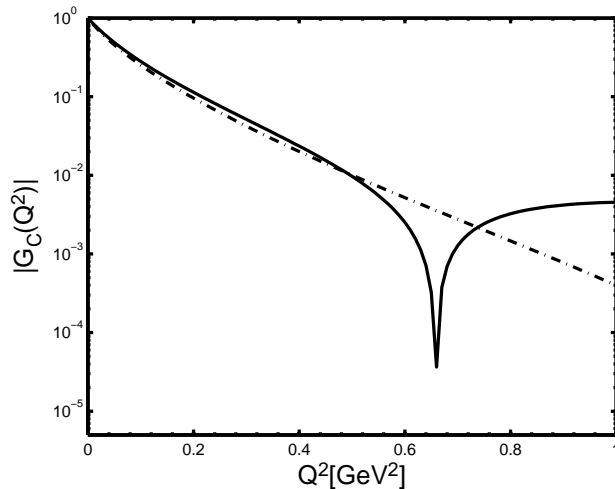


FIG. 4. Form factor $|G_C(Q^2)|$. The solid line is from the parameterizations of Ref. [29] and the dash-dotted line is our result in the light-front representation.

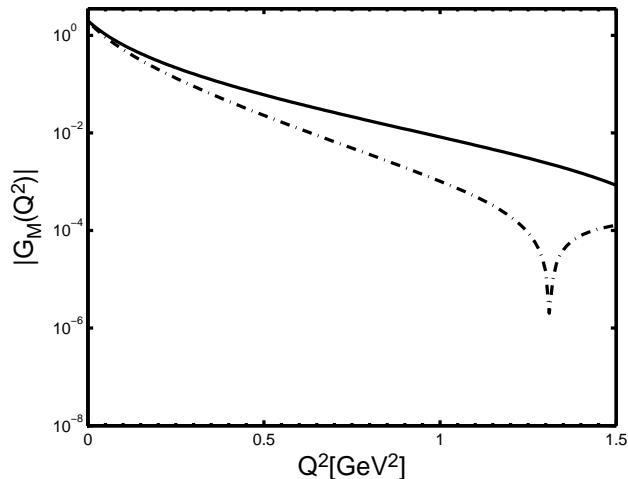


FIG. 5. Form factor $|G_M(Q^2)|$. The solid line is from the parameterizations of Ref. [29] and the dash-dotted line is our result in the light-front representation

with $J_0(qb)$ being a cylindrical Bessel function and $Q^2 = -q^2 = \vec{q}^2$. In Fig. 8 we plot the transverse charge density $\rho_C(b)$ for the proton and neutron for an example.

From Fig. 6, one can see that our result fits the one of the parametrization only qualitatively, and one can also find that different parametrizations have different results at $b = 0$ (see red solid and black dashed curves). The red solid line (black dashed line) gets the maximum value 0.720 (0.426) at $b = 0$, and our black solid line gets the maximum value 0.324. The remarkable differences are because the parametrizations are from the fit to the experimental data in the low Q^2 region, which corresponds to large b region. Therefore, for the small b region, the uncertainty is expected to be large since our knowledge for the form factors in the large Q^2 region is limited.

We can determine the deuteron mean-square transverse charge radius. It is defined as

$$\langle b_C^2 \rangle = \int d^2 b b^2 \rho_C(b), \quad (27)$$

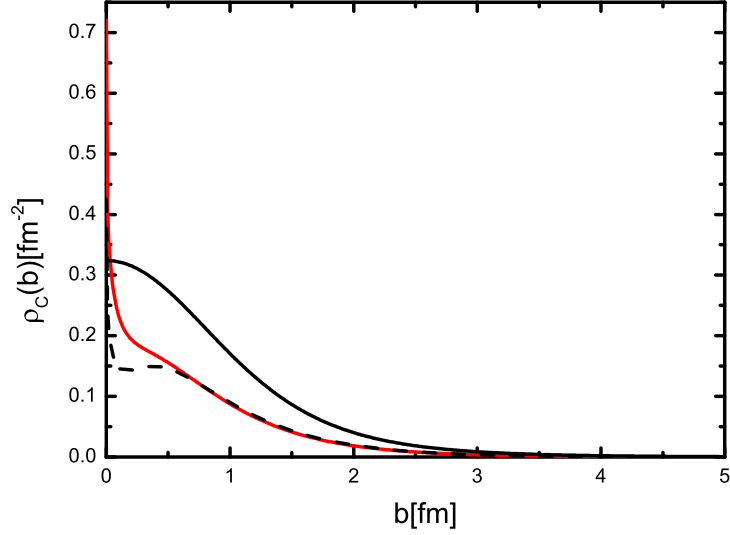


FIG. 6. The transverse charge density of deuteron. The red solid line and the black dashed line are the results of the parameterizations, the black solid line is our result in the light-front representation.

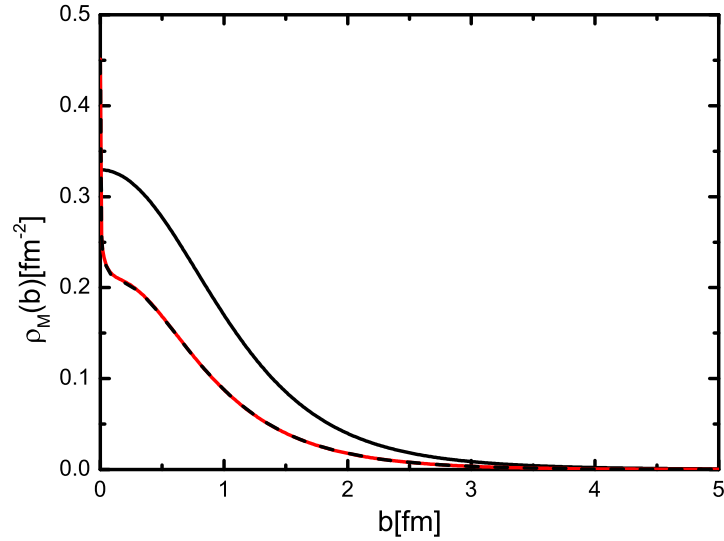


FIG. 7. The transverse magnetic density of deuteron. The red solid line and the black dashed line are the results of the parameterizations, the black solid line is our result in the light-front representation.

and it can also be yielded from

$$\lim_{Q^2 \rightarrow 0} G_C(Q^2) = 1 - \frac{Q^2}{4} \langle b_C^2 \rangle. \quad (28)$$

It stands for the size of the deuteron in the transverse plane. This quantity differs from the well-known effective mean-square charge radius R^{*2} in the three-dimension space of

$$\lim_{Q^2 \rightarrow 0} G_C(Q^2) = 1 - \frac{Q^2}{6} R_C^{*2}. \quad (29)$$

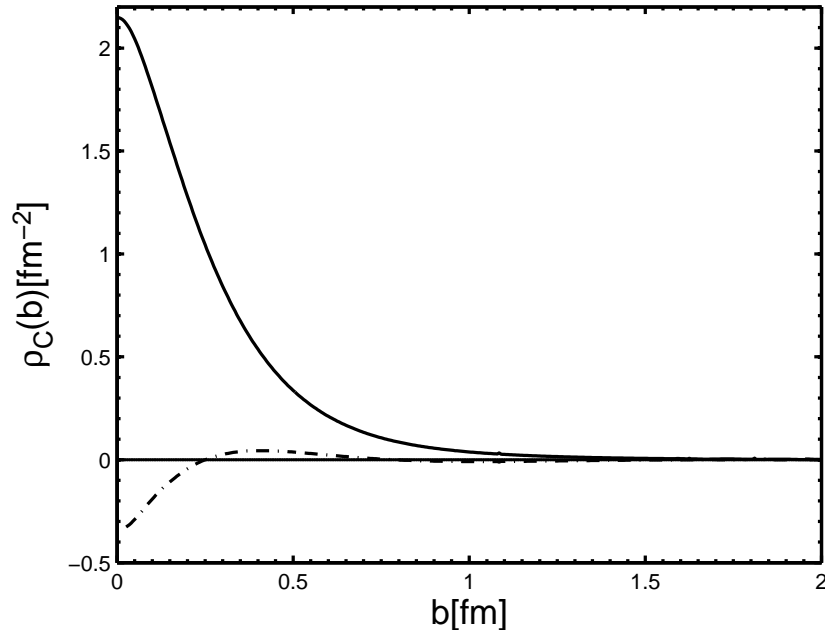


FIG. 8. The transverse charge density of proton and neutron. The solid line is the transverse charge density of proton and the dotted-dashed line is the transverse charge density of neutron.

The relation of the two quantities is $\langle b_C^2 \rangle = \frac{2}{3} R_C^{*2}$ [30]. In our calculation, we obtained $R_C^* \sim 2.75 fm$, which is consistent with the value of $R_C^* \sim 2.56 fm$ from the parameterizations [29] and the experimental extraction of $R_C^* = 2.128 \pm 0.11 fm$ [31]. The magnetic radius we obtained is about $R_M^* \sim 2.16 fm$ which also reasonably fits the result from the parameterizations of $R_M^* \sim 1.93 fm$ and the experimental data of $R_M^* = 1.90 \pm 0.14 fm$ [31].

The obtained $\rho_{C,M}(b)$, in Figs. 6 and 7, tell that they have similar b -dependences to the parameterized ones. Although the discrepancies exist in the small b region which corresponding to large Q^2 regime, they both show the peaks in the central b and a long tail in the region of large b . Conventionally, if we consider the three quark core $|3q\rangle$ in the proton or neutron, the core is always located in the central b and the size of the core is expected to be smaller than $0.5 fm$. When the meson cloud, pion meson cloud for example, is considered, the proton has the components of $|(3q)^0 \pi^+\rangle$ and $|(3q)^+ \pi^0\rangle$ and the neutron has the components of $|(3q)^+ \pi^-\rangle$ and $|(3q)^0 \pi^0\rangle$. Therefore, the long positive tail of the proton transverse charge density comes from the charge pion cloud and on the contrary, the long negative tail of the neutron transverse density results from the negative pion cloud (see Fig. 8). Here for the deuteron case (see Fig. 6), the long positive tail is expected from the positive charged pion cloud [30]. The contribution from the neutron negative pion cloud is less important and it is canceled by the contribution of the proton. Moreover, the positive peak of the transverse charge density at central b is smaller than the proton, since the contribution of the positive proton peak is partly canceled by the negative peak of the neutron and moreover the loop integral also suppresses the peak. So far, the origin of the negative peak of the neutron transverse charge density is still an open question [30].

V. SUMMARY

To summarize this work, we use a phenomenological effective Lagrangian approach to study the EM form factors of the deuteron, particularly, the transverse charge and magnetic densities of the deuteron. We show the EM form factors of the deuteron and their transverse densities in the light-front representation. We find that the present approach could reproduce the EM form factors, at least qualitatively, although it is simple with only one parameter. The important issue, in this work, is the study of the transverse densities, particularly of the transverse charge density of the deuteron. We find the transverse charge density reaches its maximum at the central b and it has a long positive tail. It means that the charge quark core is located at the central b and in the large b region, the positive charge

pion cloud dominates. This phenomenon is similar to the proton case. Moreover our analysis shows the remarkable differences between the two different parametrizations in the central b region. This is due to the fact that we know much about the charge form factor of the deuteron in the low Q^2 region, but less in the large Q^2 region and the latter one corresponds to the small b region.

It should be reiterated that our present approach is simple and it can be further improved. Here our estimated charge and magnetic form factors fit the data qualitatively. We did not show the estimated quadrupole form factor of the deuteron. This is because the quadrupole form factor is sensitive to the D -wave component of the deuteron, which we did not include explicitly. A more sophisticated calculation with a more realistic description of the deuteron wave function including D -wave component is in progress.

ACKNOWLEDGMENTS

This work is supported by National Sciences Foundations of China Nos. 10975146, 11035006, 11261130 and 11165005, as well as supported, in part, by the DFG and the NSFC through funds provided to the Sino-German CRC 110 ‘‘Symmetries and the Emergence of Structure in QCD’’. YBD also thanks the Institute of Theoretical Physics, University of Tübingen for the warm hospitality and thank the support from the Alexander von Humboldt Foundation.

Appendix A: The scalar loop integral

There are some discussions about the scalar loop integral as [32, 33]

$$I(P^2, q^2, P \cdot q) = \int \frac{d^4 k}{(2\pi)^4} \frac{1}{(k^2 - M_N^2 + i\epsilon)[(k+q)^2 - M_N^2 + i\epsilon][(P-k)^2 - M_N^2 + i\epsilon]}. \quad (\text{A1})$$

In the light-front representation, $a^\pm = a^0 \pm a^3$, and $\int d^4 k = \int \frac{1}{2} dk^+ dk^- d^2 \vec{k}$, then the integral of $I(P^2, q^2, P \cdot q)$ is

$$I(P^2, q^2, P \cdot q) = \int \frac{dk^+ dk^- d^2 \vec{k}}{2(2\pi)^4} \frac{1}{k^+ (P^+ - k^+)} \times \frac{1}{[k^- - \frac{\vec{k}^2 + M_N^2}{k^+} + \frac{i\epsilon}{k^+}] [k^- - \frac{(\vec{k} + \vec{q})^2 + M_N^2}{k^+} + \frac{i\epsilon}{k^+}] [P^- - k^- - \frac{(\vec{P} - \vec{k})^2 + M_N^2}{P^+ - k^+} + \frac{i\epsilon}{P^+ - k^+}]}. \quad (\text{A2})$$

One may integrate over the upper half plane of the complex k^- , as show in Fig. 9, and one can find a non-vanishing contribution only for the case of $0 < k^+ < P^+$. Then

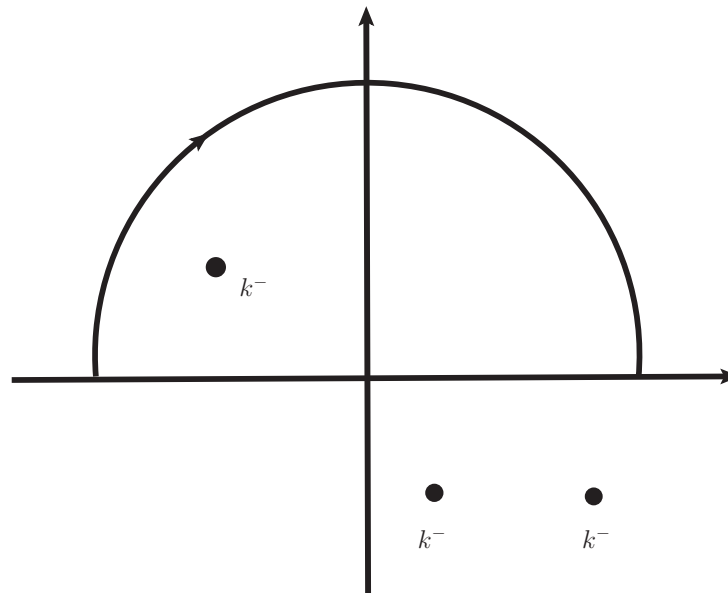
$$I(P^2, q^2, P \cdot q) = -i \int \frac{d^2 \vec{k}}{2(2\pi)^3} \int \frac{dk^+}{k^+ (P^+ - k^+)} \frac{1}{P^- - \frac{\vec{k}^2 + M_N^2}{k^+} - \frac{(\vec{P} - \vec{k})^2 + M_N^2}{P^+ - k^+}} \frac{1}{P^- - \frac{(\vec{k} + \vec{q})^2 + M_N^2}{k^+} - \frac{(\vec{P} - \vec{k})^2 + M_N^2}{P^+ - k^+}} \quad (\text{A3})$$

whereas, $k^+ < 0$ and $k^+ > P^+$ doesn't contribute to the integral.

Define $x = \frac{k^+}{P^+}$, and choosing the reference frame of $q^+ = q^- = 0$ [32, 33], then the above equation can be expressed as

$$I(P^2, q^2, P \cdot q) = -i \int \frac{d^2 \vec{k}}{2(2\pi)^3} \int_0^1 \frac{dx}{x(1-x)} \frac{1}{P^+ P^- - \frac{\vec{k}^2 + M_N^2}{x} - \frac{(\vec{P} - \vec{k})^2 + M_N^2}{1-x}} \frac{1}{P^+ P^- - \frac{(\vec{k} + \vec{q})^2 + M_N^2}{x} - \frac{(\vec{P} - \vec{k})^2 + M_N^2}{1-x}} \quad (\text{A4})$$

-
- [1] R. A. Gilman and F. Gross, J. Phys. G **28**, R37 (2002).
 - [2] I. Sick, Prog. Part. Nucl. Phys. **47**, 245 (2001).
 - [3] F. Gross, Eur. Phys. J. A **17**, 407 (2003).
 - [4] M. Garcon and J. W. Van Orden, Adv. Nucl. Phys. **26**, 293 (2001).
 - [5] R. G. Arnold, C. E. Carlson, and F. Gross, Phys. Rev. C **21** 1426 (1980), Phys. Rev. C **23**, 363 (1981).

FIG. 9. The k^- complex plane.

- [6] J. F. Mathiot, Phys. Rept. **173**, 63 (1989); H. Henning, J. J. Adam, P. U. Sauer and A. Stadler, Phys. Rev. C **52**, 471 (1995); J. J. Adam and H. Arenhovel, Nucl. Phys. A **614**, 289 (1997).
- [7] R. B. Wiringa, V. G. J. Stoks and R. Schiavilla, Phys. Rev. C **51**, 38 (1995).
- [8] H. Arenhovel, F. Ritz and T. Wilbois, Phys. Rev. C **61**, 034002 (2000).
- [9] M. Gari and H. Hyuga, Nucl. Phys. A **278**, 372 (1977); V. V. Burov, S. M. Dorkin and V. N. Dostovalov, Z. Phys. A **315**, 205 (1984); V. V. Burov and V. N. Dostovalov, Z. Phys. A **326**, 245 (1987); A. Buchmann, Y. Yamauchi and A. Faessler, Nucl. Phys. A **496**, 621 (1989); A. Valcarce, F. Fernandez, A. J. Buchmann and Amand Faessler, Phys. Rev. C **50**, 2246 (1994); H. Ito and L. S. Kisslinger, Phys. Rev. C **40**, 887 (1989); E. Hummel and J. A. Tjon, Phys. Rev. Lett. **63**, 1788 (1989).
- [10] V. A. Karmanov and A. V. Smirnov, Nucl. Phys. A **575**, 520 (1994); J. Carbonell and V. A. Karmanov, Eur. Phys. J. A **6**, 9 (1999); J. W. Van Orden, N. Devine and F. Gross, Phys. Rev. Lett. **75**, 4369 (1995); J. Carbonell, B. Desplanques, V. A. Karmanov and J. F. Mathiot, Phys. Rept. **300**, 215 (1998). D. R. Phillips, S. J. Wallace and N. K. Devine, Phys. Rev. C **58**, 2261 (1998); T. W. Allen, W. H. Klink and W. N. Polyzou, Phys. Rev. C **63**, 034002 (2001); T. W. Allen, G. L. Payne and W. N. Polyzou, Phys. Rev. C **62**, 054002 (2000); F. M. Lev, E. Pace and G. Salme, Phys. Rev. C **62**, 064004 (2000); L. L. Frankfurt and T. Frederico and M. Strikman, Phys. Rev. C **48**, 2182 (1993).
- [11] D. B. Kaplan, M. J. Savage and M. B. Wise, Phys. Rev. C **59**, 617 (1999); T. S. Park, K. Kubodera, D. P. Min and M. Rho, Phys. Rev. C **58**, 637 (1998); J. W. Chen, H. W. Griesshammer, M. J. Savage and R. P. Springer, Nucl. Phys. A **644**, 245 (1998); M. Walzl and U. G. Meissner, Phys. Lett. B **513**, 37 (2001); D. R. Phillips, Phys. Lett. B **567**, 12 (2003); S. R. Beane, M. Malheiro, J. A. McGovern, D. R. Phillips and U. van Kolck, Nucl. Phys. A **747**, 311 (2005); D. Choudhury and D. R. Phillips, Phys. Rev. C **71**, 044002 (2005); R. P. Hildebrandt, H. W. Griesshammer, T. R. Hemmert and D. R. Phillips, Nucl. Phys. A **748**, 573 (2005); D. R. Phillips, J. Phys. G **34**, 365 (2007).
- [12] A. N. Ivanov, N. I. Troitskaya, M. Faber and H. Oberhummer, Phys. Lett. B **361**, 74 (1995).
- [13] M. Lacombe, B. Loiseau, R. Vinh Mau et al., Phys. Lett. B **101**, 139 (1981); R. Machleidt, Phys. Rev. C **63**, 024001 (2001).
- [14] W. W. Buck and Franz Gross, Phys. Rev. D **20**, 2361 (1979); F. Gross, J. W. Van Orden and K. Holinde, Phys. Rev. C **45**, 2094 (1992); J. J. Adam, F. Gross, S. Jeschonnek, P. Ulmer and J. W. Van Orden, Phys. Rev. C **66**, 044003 (2002); F. Gross and A. Stadler, Phys. Rev. C **78**, 014005 (2008); F. Gross and A. Stadler, Phys. Rev. C **82**, 034004 (2010).
- [15] J. Carbonell and V. A. Karmanov, Nucl. Phys. A **581**, 625 (1994); V. A. Karmanov, Nucl. Phys. A **362**, 331 (1981).
- [16] L. L. Frankfurt and M. I. Strikman, Nucl. Phys. B **148**, 107 (1979); L. A. Kondratyuk and M. I. Strikman, Nucl. Phys. A **426**, 575 (1984); L. L. Frankfurt, T. Frederico and M. Strikman, Phys. Rev. C **48**, 2182 (1992).
- [17] D. E. Soper, Phys. Rev. D **5**, 1956 (1972).
- [18] M. Burkardt, Int. J. Mod. Phys. A **18**, 173 (2003).
- [19] M. Diehl, Eur. Phys. J. C **25**, 223 (2002) [Erratum-*idid.* C **31**, 277 (2003)].
- [20] C. E. Carlson and M. Vanderhaeghen, Phys. Rev. Lett. **100**, 032004 (2008).
- [21] G. A. Miller, Phys. Rev. Lett. **99**, 112001 (2007), G. A. Miller, Phys. Rev. C **79**, 055204 (2009).
- [22] S. Weinberg, Phys. Rev. Lett. **18**, 188 (1967); Phys. Rev. **166**, 1568 (1968).
- [23] A. Salam, Nuovo Cim. **25**, 224 (1962).
- [24] K. Hayashi et al., Fortschr. Phys. **15**, 625 (1967).

- [25] G. V. Efimov and M. A. Ivanov, “The quark confinement model of hadrons”, (IOP, Bristol, 1993)
- [26] Y. B. Dong, A. Faessler, T. Gutsche, and V. E. Lyubovitskij, Phys. Rev. D **77**, 094013 (2008); Y. B. Dong, Amand Faessler, T. Gutsche, S. Kovalenko, and V. E. Lyubovitskij, Phys. Rev. D **79**, 094013 (2009) Y. B. Dong, A. Faessler, T. Gutsche, and V. E. Lyubovitskij, J. Phys. G **38**, 015001 (2011); Phys. Rev. D **81**, 014006 (2010); *idid* D **81**, 074011; Y. B. Dong, A. Faessler, T. Gutsche, S. Kumano, and V. E. Lyubovitskij, Phys. Rev. D **82**, 034035; *idid* D **83**, 094005; Y. B. Dong, A. Faessler, T. Gutsche, and V. E. Lyubovitskij, J. Phys. G. **40**, 015002 (2013); Y. B. Dong and Y. Z. Wang, J. Phys. G **39**, 025003 (2012).
- [27] Y. B. Dong, Amand Faessler, Thomas Gutsche and V. E. Lyubovitskij, Phys. Rev. C **78**, 035205 (2008); Y. B. Dong, Phys. Rev. C **80** 025208 (2009); Yubing Dong and Cuiying Liang, J. Phys. G. **40**, 025001 (2013).
- [28] Yubing Dong and S. D. Wang, Phys. Lett. B **684**, 123 (2010); Y. B. Dong, Phys. Rev. C **81**, 018201 (2010).
- [29] E. Tomasi-Gustafsson, G. I. Gakh and C. Adamuscin, Phys. Rev. C **73**, 045204 (2006).
- [30] G. A. Miller, Phys. Rev. Lett. **99**, 112001 (2007); G. A. Miller, Ann. Rev. Nucl. Part. Sci., **60**, 1 (2010).
- [31] Andrei Afanasev, V. D. Afanasev and S. V. Trubnikov, “Magnetic Radius of the deuteron”, 9808047 [nucl-th].
- [32] Bruno El-Bennich, J. P. B. C. de Melo and T. Frederico, Few-Body Systems **54**, 1851 (2013).
- [33] G. A. Miller, Phys. Rev. C **80**, 045210 (2009).
- [34] P. G. Bunden, W. Melnitchouk and J. A Tjon, Phys. Rev. C **72**, 034612 (2005).